Geosciences 2013, 3(4): 128-141
DOI: 10.5923/j.geo.20130304.04

Subduction Related Magmatism: Constrains from the REE Pattern in the Lohit Batholith, Arunachal Pradesh, India

Tapos Kumar Goswami

Department of Applied Geology, Dibrugarh University, Dibrugarh, Pin: 786 004 Assam, India

Abstract The Trans Himalayan Lohit batholith in the eastern part of Arunachal Pradesh is dominantly quartz dioritic in the southwestern part while the north eastern part is intruded by leucogranite dykes. This study reports the major and trace element geochemistry of dominant intrusive phases along Lohit and Dibang river valleys of eastern Arunachal Pradesh. The petrographic and geochemical studies characterize these rocks as typical metaluminous I-type granites with occasional mafic (gabbroic) enclaves in the southwestern part. The north east part of the batholith shows fractionated and evolved and weakly peraluminous granites. The rocks show heterogeneous Sr isotopic ratios varying from 0.703876 to 0.714698 from south west to north eastern part of the batholith. The observed geochemical data also indicate dominant cal-alkaline character of the rocks. There is a gradual increase of LILE and depletion HREE from the gabbro-quartz diorite sequence to leucogranite with higher values of Si and decrease of Fe, Mg, Y, Yb. The quartz diorites and the enclaves of gabbro are co genetic in nature with low Ce/Yb ratios. The $(La/Yb)_N$ ratios for gabbro indicate varying degree of partial melting and stabilization of garnet in the source. Involvement of subducted tonalitic sediments with the crustal melt may be responsible for the absence of Eu anomaly in biotite leucogranites. The study indicates at least two magma source components involved in the petrogenesis: (1) less differentiated mantle-wedge mafic magmas assimilated by lower crust of the Asian continent and (2) more evolved magma from the melting of the upper continental Asian crust in the northeastern part.

Keywords Lohit Batholith, Subduction, Magmatism, Geochemistry, REE Patterns

1. Introduction

The Himalayan Mountain is the unique example of the youngest continent to continent collision tectonics. The boundary between the Indian and Eurasian plate is marked by the Indus-Tsangpo Suture zone. To the north of the suture zone, the trans- Himalayan batholith runs almost the entire length of Himalaya from NW, through the Nepal Himalaya and to the Myanmar to the east. The batholith from NW to NE is variously named as Kohistan batholith in Pakistan, Gangdese batholih in south Tibet and Lohit batholith in Arunachal Pradesh[22, 26, 53, 44]. These Trans- Himalayan batholiths of calc-alkaline nature are intrusives on the southern edge of the Eurasian plate in the immediate north of the ITSZ. The batholiths occur in a linear belt for about 2500km and 20-80km wide zone and represent an Andean type magmatism of the Tethyan oceanic crust under Eurasian plate during late Cretaceous to Lower Eocene time[19,47]. Compositional variety of these batholiths ranges from gabbro to granite although biotite and hornblende bearing granodiorite dominates in most part. The batholiths are I-type Cordilleran batholith and probably emplaced during 100-40 Ma, the dominant phase being intruded at 60Ma[21]. Nd, Sr and Pb isotopic compositions of Ladakh and Gangdese batholith indicate predominantly their mantle derivation and U-Pb ages vary between 105 -45 Ma for these batholiths[43]. The magma genesis, age relationships and emplacement history of Ladakh and Gangdese batholiths are widely discussed[3, 8, 9, 10, 38, 51]. However, the Lohit batholith of Arunachal Pradesh did not get much attention and only a few published data are available[46, 40, 26, 15, 16]. The Lohit batholith is located in the eastern part the Arunchal Pradesh at the eastern limb of the eastern syntaxis. The batholith is about 100km in width and has a NW-SE extension of about 250km[35] and extends from Tuting in the upper reaches of Siang river, through upstream segments of Dibang and Lohit river and extends further in the south -east direction (Fig. 1). In the south western part, the batholith is thrusted on the Tuting –Tidding suture zone, which is considered as the continuation of the Indus Tsangpo Suture Zone to the south east direction[47,13, 34, 2, 44, 15,17]. The batholith was studied initially by only a few workers because of the inhospitable terrain and poor

* Corresponding author:
taposgoswami@yahoo.com (Tapos Kumar Goswami)
Published online at http://journal.sapub.org/geo
Copyright © 2013 Scientific & Academic Publishing. All Rights Reserved

communication facilities. Previous studies have thrown some light on the geology and geochemistry of the Lohit batholith[46, 47, 40, 15, 16]. This paper highlights the subduction related magmatism of the Tethyan oceanic crust under western edge of the Burmese plate on the basis of major and REE geochemistry in the Lohit batholith.

Outline geology of Lohit batholith

The eastern Himalayan syntaxis consists of three tectonic units: (1) the Himalayan part in the south west (ii) the Tuting-Tidding Suture Zone (TTSZ) and (iii) the magmatic part in the north east, named as the Lohit batholith (Fig.2). The Lohit batholith is thrusted over the TTSZ along the Lohit Thrust[35]. The TTSZ represent the neotethyan oceanic crust and encompasses various lithologies like actinolite-schist, chlorite–quartz-phyllite, graphite-phyllite, crystalline limestone, garnetiferous amphibolite and dykes and sills of serpentinite. The litho-package of the TTSZ shows NE dipping imbricate faulting and has a thrust contact with the Himalayan belt in the south west[42, 1, 16, 12]. The suture belt has a NW-SE extension and in the NW part, it is traceable as continuous belt in the upstream part of the Dibang river, however, it is again discontinuous in the further NW direction and reappears at Tuting, the upper reaches of the Siang river. The batholith is about 100km in thickness in the Lohit valley; however along the NW direction the thickness is reduced to about 70 km in the Dibang valley and further reduced along the Siang valley. An Andean type of calc -alkaline magmatism is represented by the batholith due to the subduction of the neo -tethyan oceanic crust beneath the Eurasian plate. The timing of the subduction, whether late cretaceous or early Eocene is yet to be constrained.

Quartz diorites are volumetrically more significant in the Lohit batholith especially in the southwestern part. These are dominated by hornblende, plagioclase, quartz and biotite. The mafic constituents are more than 20 percent of the bulk rock. The quartz diorites show subhedral granular texture with sphene, apatite, zircon and iron oxides occurring as accessory phases. Hornblende dominated varieties are hornblende- biotite diorites. Alteration of hornblende to biotite is observed. The K-feldspar poor varieties grade in to tonalite while the K-feldspar bearing varieties are granodiorites. Gabbro occurs as enclaves consisting of plagioclase and pyroxene phenocrysts. Trondhjemites occur as tabular bodies and composed of Na rich plagioclase, quartz and biotite. Towards the eastern part of Chingawanti, granodiorites are observed, which grade in to granites on the basis of model mineralogy. K-feldspars in these rocks are coarse and frequently show fracturing due to brittle deformation. Biotite, hornblende and opaques constitute the mafic phase. Eastern part of the batholith, both in Lohit and Dibang valleys, is dominated by leucogranites. In the Lohit valley near Yasong and in the Dibang valley in Dambwen, leucogranites are observed to be intruding the earlier quartz diorites. Leucogranites are mainly composed of quartz, K-feldspar, plagioclase, biotite, muscovite, epidote and garnet. Both varieties of K-feldspar are found in leucogranite, however, orthoclase is dominant compared to plagioclase. Mafic minerals constitute <5% of the bulk rock in the leucogranites. The sillimanite schist of the Yasong area in the Lohit valley should represent the host rock lithology. The prismatic sillimanite and biotite flakes define the foliation. The foliation occasionally wraps around garnets. In some leucogranites, quartz appears as equent strain free grains. Among the acid intrusives, dacite and rhyolite dominates, consisting k-feldspar, plagioclase and quartz phenocrysts.

2. Petrography

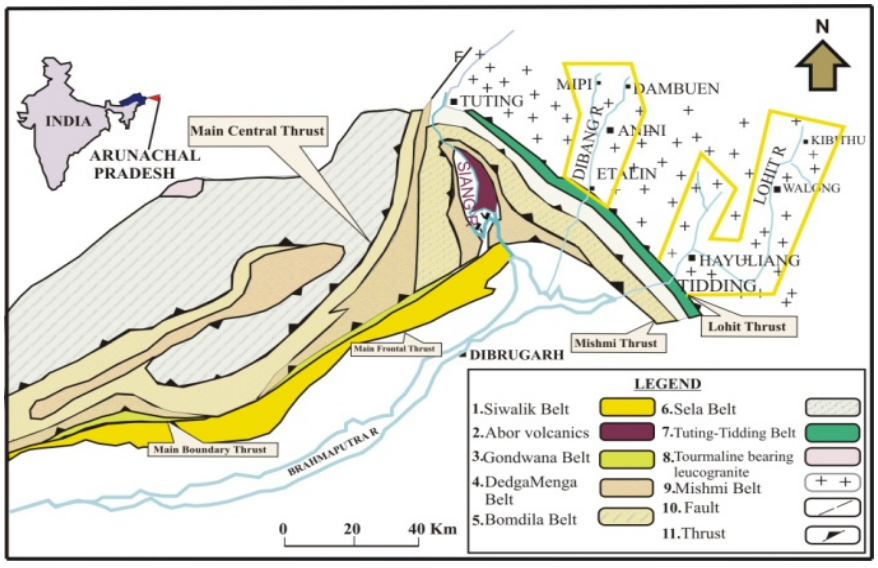

Figure 1. Geological map of Arunachal Pradesh modified from Singh and Chowdhury (1990)[42]. 1. Siwalik Belt 2. Abor volcanics 3.Gondwana belt 4.Dedga Menga Belt. 5. Bomdila Belt 6.Sela Belt 7.Tuting–Tidding Belt 8. leucogranite 9.Mishmi belt 10. Fault 11. Thrust. The extent of the investigation in the two river sections are bordered

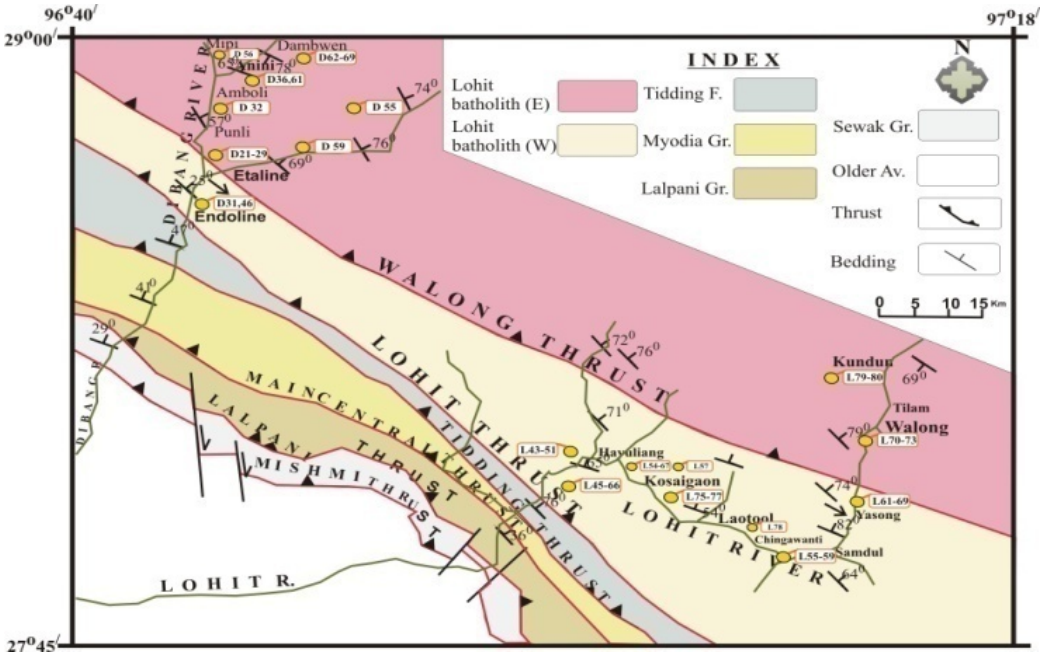

Figure 2. Geological map of area (modified after Mishra, 2009[33] ; Gururajan and Chowdhury, 2007)[15]. The investigation is carried out in the Lohit and Dibang valleys beyond Tiding Thrust. Sample locations of rock types are shown for Lohit (starts with L) and Dibang valley (starts with D) as per the Tables 1a-1d

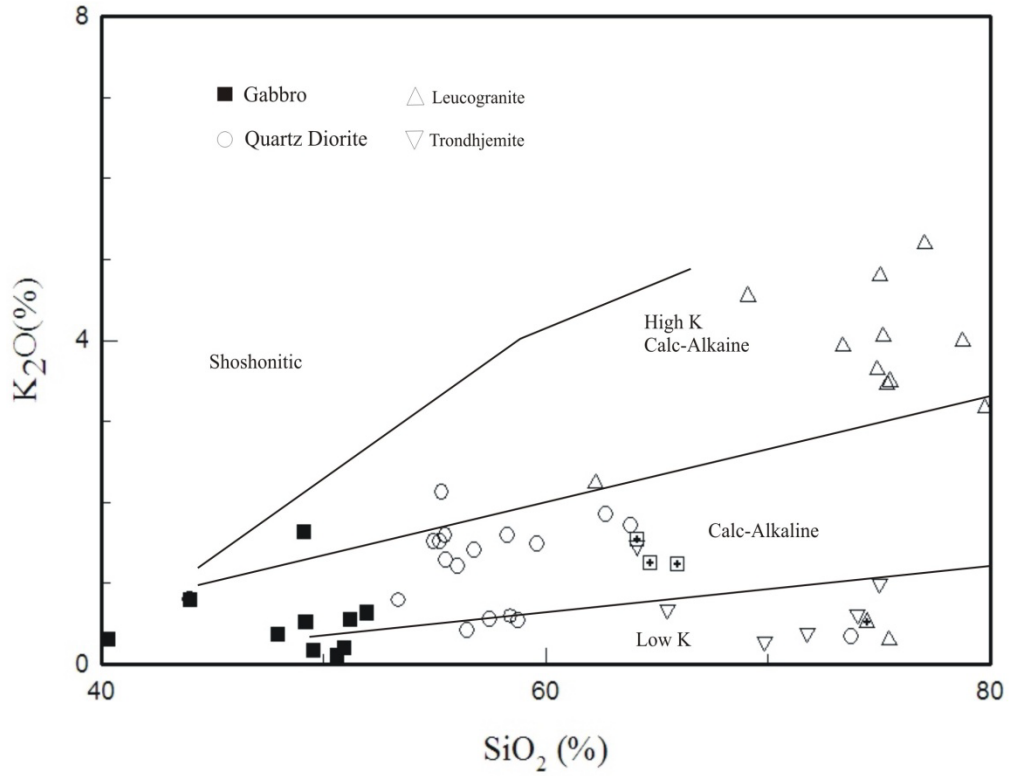

Figure 3. K_2O versus SiO_2 binary diagram of Lohit batholith using the classification scheme of Peccerillo and Taylor (1976)[37]

3. Geochemistry

3.1. Sampling

Samples of gabbro, quartz diorite, trondhjemite and leucogranites are collected from both of the Lohit and Dibang valleys. In the Lohit valley, starting from Payapani up to Lautool, both gabbro and quartz diorites are collected while trondhjemites are collected from Chingawanti. Quartz diorites are exposed even beyond Walong up to Tilam (Fig.2). Leucogranites are collected 1km north east of Samdul to 1.5km northeast of Yasong. In the Dibang valley, gabbro and quartz diorites are collected from Angolian up to Anini while quartz diorites are exposed up to Dambwen and Mipi and samples are collected from different locations

along these two sections (Fig.2). Trondhjemites are collected from Angolian. Leucogranites are exposed from 2km SSW of Dambwen along the Dri river valley and samples are collected along this route up to Dambwen (Fig.2).

3.2. Analytical Techniques

About 50 fresh unweathered samples are ground to make fine powder in a tungsten ball mill grinder. These samples are analysed for major, trace and rare earth elements (REE) at Wadia institute of Himalayan Geology, Dehradun, India. Geochemical analyses were performed using standard XRF techniques, analysed by wavelength dispersive XRF system (Siemens SRS 3000). The calibration of the XRF system was done by matrix correction based on intensities[28]. International standards used are JG1 and JG 2 and quality of the analysis was monitored. Analytical accuracy on XRF is better than 5% for major oxides and 12% for trace elements and precession on maximum observed standard deviation is better than 2%[41]. The set of 50 samples also analysed for REE using ICP-MS (Perkins –Elmer SCIEX) with 0.6 g of the sample following a procedure of acid digestion that involved repeated treatment with HF-$HCLO_4$ in the ratio 2:1. Dissolved samples in the acid mixture underwent two or three treatments until a clean solution is obtained. The residue is than dissolved in 1N HNO_3 and 100ml solution is than ready for analysis. The relative standard deviation (RSD) for most REE analysed on ICP-MS is better than 10%[24]. Geochemical values for major trace and REE for each individual rock type are given in Tables 1a-d.

3.3. Major Element Geochemistry

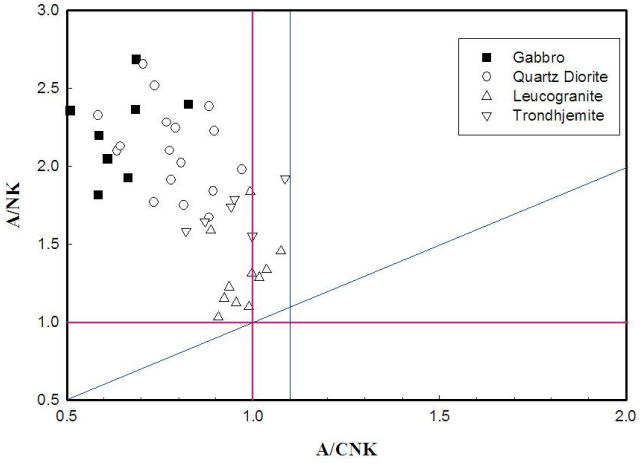

Figure 4. A/CNK versus A/NK plots of Lohit garnitoids (Shand 1927)[39]

Geochemical data for the different rock types of Lohit batholith are limited[42,16].Although the Lohit valley is studied in the previous studies, the Dibang valley, specifically its upstream section is not well covered. In the present study both the Lohit and Dibang valleys are exhaustively covered. Samples of gabbro, quartz diorites, trondhjemites, leucogranites, dacites and aplites were selected for geochemical analysis. However, considering the limited occurrences of dacites and aplites, most of the geochemical characterization is based on the other major rock types of the area.

Gabbro, quartz diorites, trondhjemites and leucogranites form the bulk of the composition of the batholith with SiO_2 content showing a considerable range (~40-80 wt%). All samples belong to low to medim K calc-alkaline rocks on a classification diagram[37] (Fig.3). However, a few samples of leucogranite also plot in the high –K alkaline field. In the ASI discrimination diagram the granitoid plot dominantly in the metaluminous field, where as some leucogranites also plot on the I-S line (Fig.4).

The A/CNK (molar ratio of Al_2O_3/ ($CaO+Na_2O+K_2O$) varies from 0.42 to 1.08. Almost all the samples contain biotite and hornblende and therefore belong to I-type granitic rocks[7]. Major element composition of different rock types are characterized by variable amounts of SiO_2, low to medium contents of K_2O, high content of Al_2O_3 and high Na_2O/K_2O ratios. Plotting together, their TiO_2, MgO, CaO, Al_2O_3, MnO, Fe_2O_3 and P_2O_3 decreases while K_2O and Na_2O increase with increasing silica content. In the total alkali silica diagram (TAS) the composition of the granitoid range from gabbro to granite with dominance in the diorite field (Fig.5). Major element in trondhjemites however gives a different concentration pattern. With the SiO_2 wt% varying from ~64 to 75 wt% , Al_2O_3 is varying within a narrow range of ~15 to 18wt%. These rocks are medium K in nature and Na_2O> 3.30 wt% and Na_2O/ K_2O >2 except sample L59. These medium K rocks are weakly peraluminous with A/CNK value close to 1 and greater than 1 in case of L59. In all of these samples MgO is less than 1. Granites of Yasong area are characterized by very high SiO_2 (65.25-80.12 wt%). Compared to gabbro, quartz diorites and trondhjemites, K_2O value in these granites is high which increase with increasing silica content, whereas MgO, CaO and TiO_2 continually decrease indicate they are weakly peraluminous. The plots are straddling the line dividing I-type and S-type granites.

3.4. Trace Element Geochemistry

The gabbro enclaves show lower concentration of lithophile elements (Rb, Ba, Th, Sr) and REE.

Transitional elements like Ni is higher in concentration while there is a significant depletion in Nb. Incompatiable elements like Ba and Th show slight enrichment and depletion of Rb is significant (Table2a-d). The $(La/Yb)_N$ ratio varies between 0.61 to 8.48 and no significant Eu anomaly is observed[25]. Nb and Zr depletion is evident in the sample versus primitive mantle spidergram (Fig.6a) where as Ta and Hf contents are also low in gabbro (ESM Table 1A).

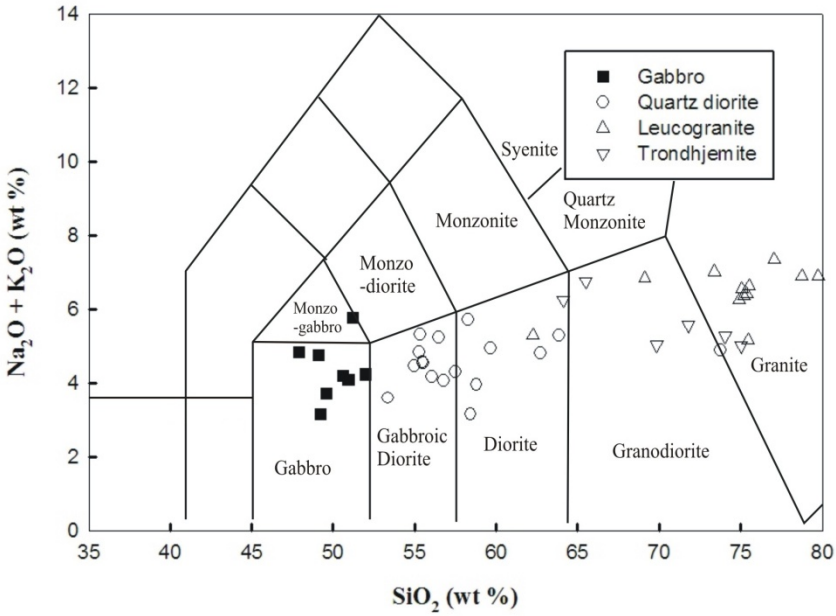

Figure 5. TAS classification diagram of the granitoids using the classification scheme of (TAS Middlemost Plot)[31]

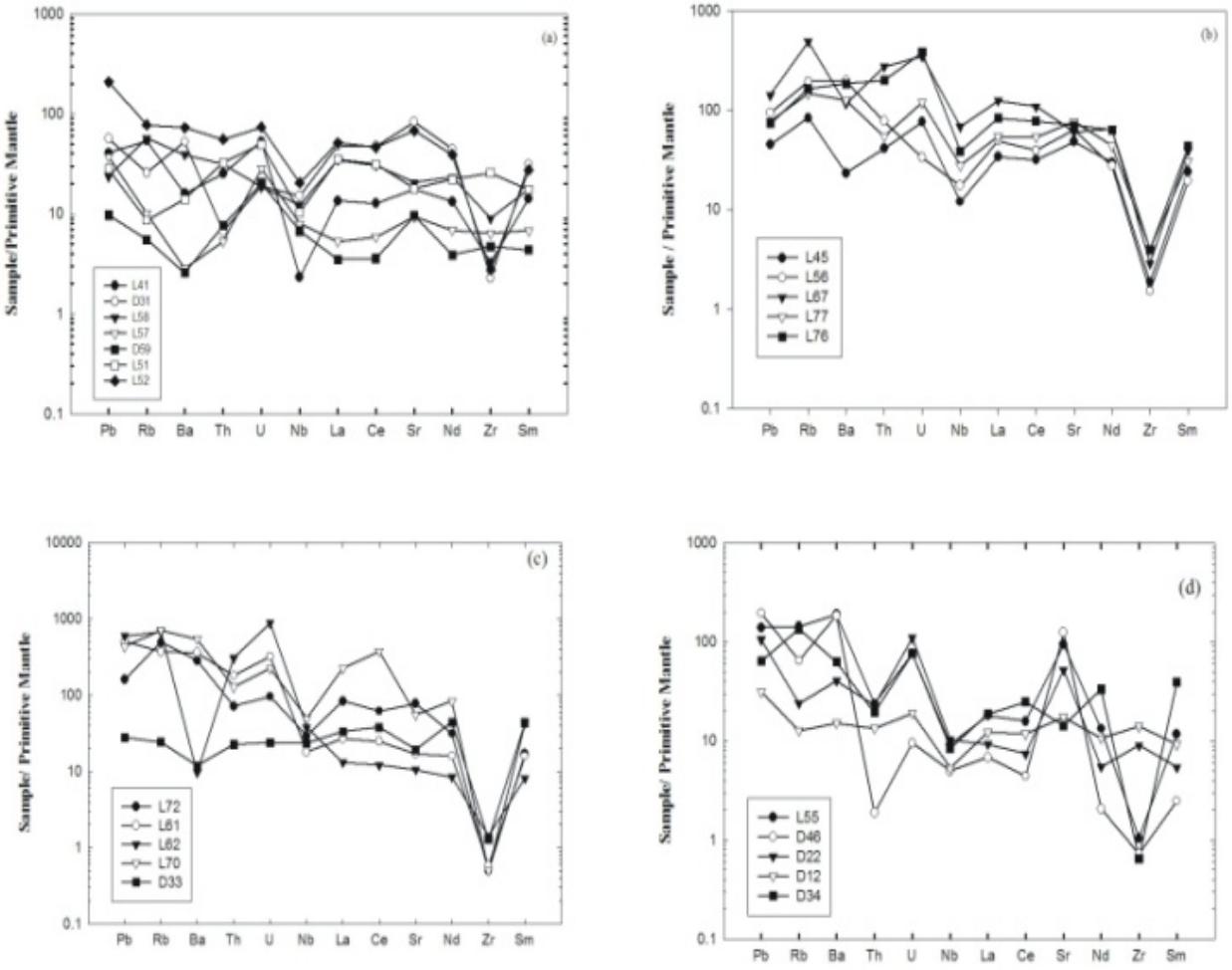

Figure 6. a-d Mantle normalized spidergram for (a) Gabbro (b) quartz diorite (c) leucogranite (d) trondhjemite

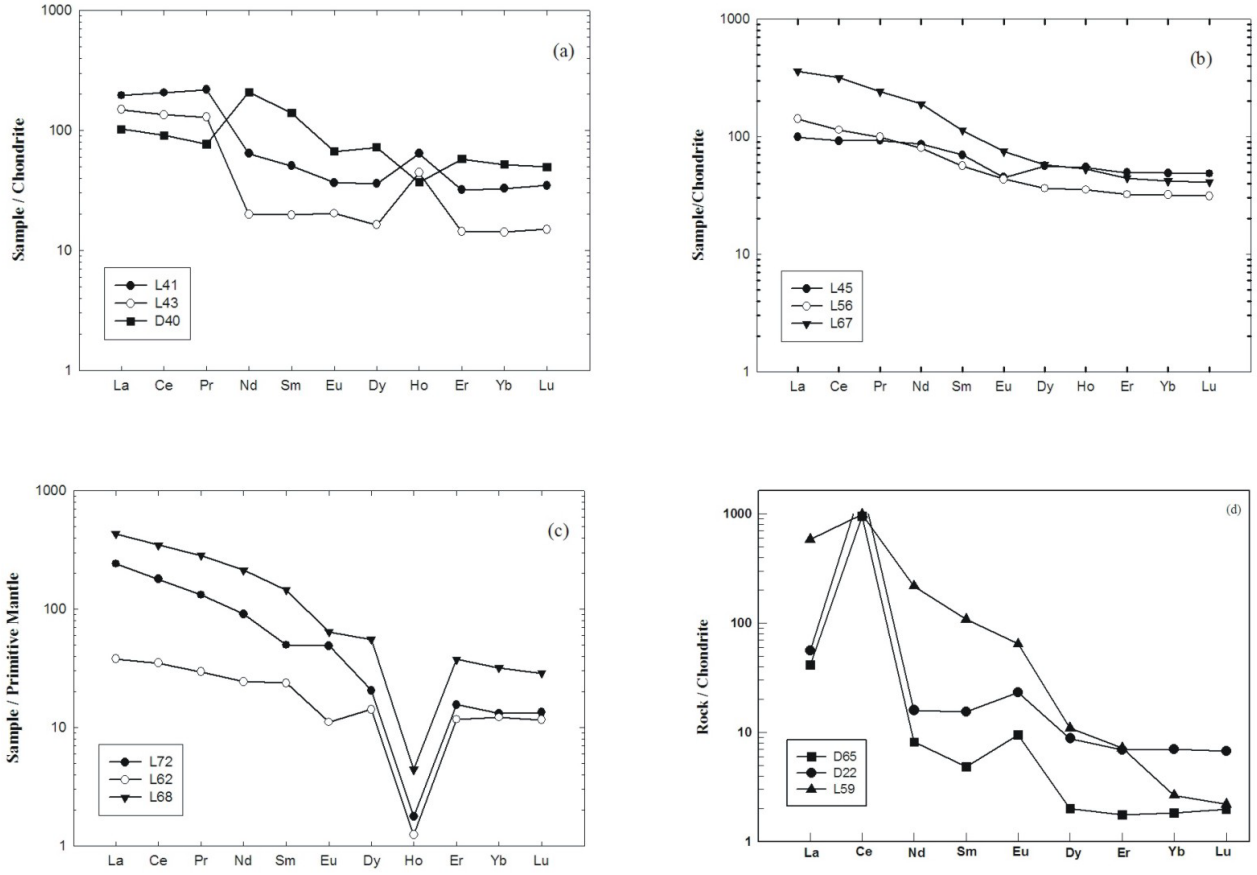

Figure 7. a-d.Chondrite normalized spidergram for (a) gabbro (b) quartz diorite (c) trondhjemite (d) leucogranite

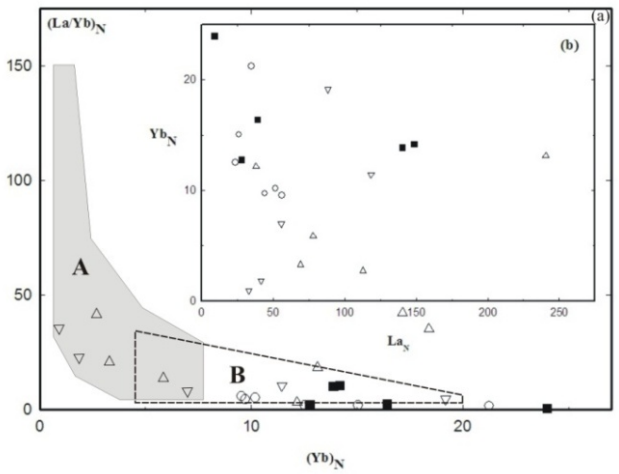

Figure 8. Chondrite normalized La/Yb ratios vs.Yb for Lohit granitoids. Fields of (A) adakite and TTG and (B) calc- alkaline lavas are from Martin (1999)[29]. Symbols as in Figs.3-5

The trace element composition of quartz diorites are characterized by high concentration of Sr and low concentration of Yb (Table 2a-d). In the primitive mantle multi element spidergram there is an increase of Nb, Ba, Rb and Sr in the quartz diorites corresponding to increase in silica (Fig.6a-d). Decrease of Nb with increase in silica and higher concentration of Sr in quartz diorites compared to gabbro is also observed (Figs.6b and 7b). Increase in Ba, Pb, Sr and depletion of Th, Nb and Zr are also observed in the spidergrams. Hf and Ta depletion in quartz diorites compared to gabbro is also observed[48]((ESM Table). Trondhjemites show a different fractionation pattern and are characterized by high (La/Yb)N ratios (~36-4.61) and low Primitive mantle normalized spidergram indicates that large ion lithophile elements like Rb, Ba, Sr and U and Th are higher in these rocks. Low values of Nb and Zr are evident from the spidergram. The (La/Yb)N (0.92-49.79) with two sample showing exceptionally high values 122.08 and 219.16 also supports the fact that leucogranites may be derived from the crustal melts. Heavy REE (HREE e.g. Yb varies between 0.16 and 0.19) and are therefore remarkably different from other cal alkaline rocks of the area (Figs.6d an7d). The high Sr content (583 – 2634.82ppm) and low Yb (0.16 -1.94 ppm) and low Eu anomaly point towards their geochemical characteristics similar to adakites[19, 23].

3.5. Sr Isotopes

Whole rock Rb $_{(ppm)}$, Sr $_{(ppm)}$, ^{87}Rb / ^{86}Sr $_{(atomic)}$ and $^{87}Sr/^{86}Sr$(atomic) are presented for eight sample of the Lohit batholith in the Table-2. These analysis were carried out at Institute Instrumentation centre, IIT Roorkee, India using techniques described by[48, 49]. Present day $^{87}Sr/^{86}Sr$ shown in the Table.2 indicates that the Sr isotopic ratio in the quartz diorites of the south western part (0.703876±0.0003 sample L45) is increasing considerably in leucogranites (0.714987 ±

0.0001 sample L69). This increase in Sr isotopic ratio can be well correlated with the continual increase in LILE and decrease of HREE and HFSE in the granitoids of Lohit batholith from southwestern to north eastern part.

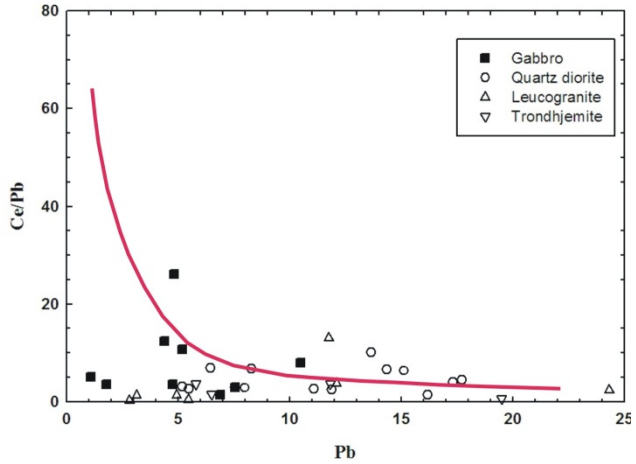

Figure 9. Ce/Pb versus Pb diagram. The trend showing continuous increase of Pb in OIB, E-MORB and increase in Ce in the granite is superimposed from Gursu, 2008[17]. Symbols as in Figs.3-5

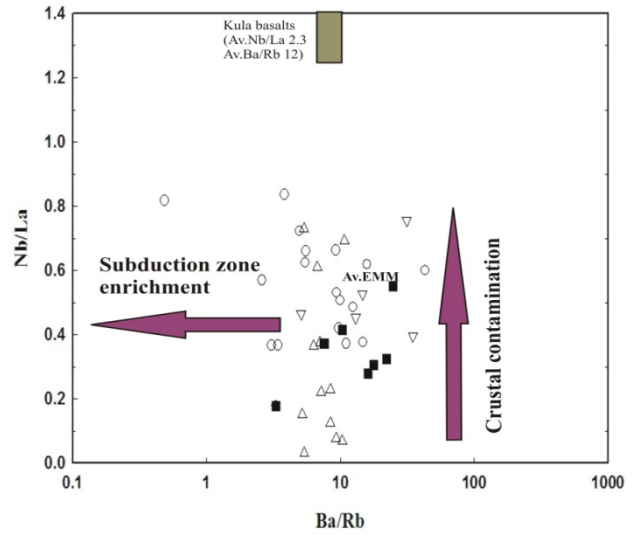

Figure 10. Nb/La versus Ba/Rb diagram illustrating the effects of crustal contamination and subduction metasomatism during the evolution of Lohit batholiths (EMM: Averaged Enriched mantl melts Yang et al 2004[52]; Altunkayanak et al 2010[5]; Kula basalts: Dilek and Altunkayanak (2010)[11]. Symbols as in Figs.3-5

4. Discussion

4.1. REE Patterns

In general various intrusive phases in the Lohit batholith show a gradual LILE enrichment and HREE depletion with the increasing silica content. Gradual enrichment of Ba, Sr, Pb and low contents of Yb, Zr and Nb can be studied from the spidergrams (Figs.6a-d and 7a-d). La/Yb ratio increases from early intrusives of gabbro and quartz diorites to the leucgranites. The depletion of Nb, Zr, Hf and Ta in the mafic enclaves and host quartz diorites indicate that the melt was derived from enriched lithospheric mantle contaminated by ancient crustal material[52, 54]. On the other hand, negative anomalies are shown by Ba, Sr and Nb in leucogranites, which have high values of Rb, Th and La (Fig.6.c). These features are compatible to (i) crustally derived melts (ii) partial melting of acid to intermediate igneous rocks or (iii) melting of immature type of sediments for the formation of leucogranites[50]. Trondhjemites are characterized by high $(La/Yb)_N$ (4.61 to 35.55) $(Yb)_N$ (0.94 to11.43). These characteristics place them in the adakite or TTG fields (Fig.8).

Considering the low Ce/Pb ratio[32] (Fig.9), Pb enrichment in the granitoids may be derived from the oceanic crust by fluids adding to the mantle wedge before melting[30]. This mantle Pb may be transferred to the arc magma source before its melting. The fig. shows the plots of this study which can be compared with the Ce/Pb ratios in the Oceanic basalts and Continental crust[31]. Pb enrichment is therefore similar to the enrichment of Rb or U despite being the fact that Pb is moderately compatible in comparison to Rb and U. On the other hand Ce/Pb –Pb variations indicate that Pb may also be added by magmatic differentiation of intracrustal meting of a TT source that is in the garnet stability field under the mantle wedge[14]. This ratio also supports a two component mixing process between the magma derived from a moderately enriched mantle source and a sedimentary component[18].

Trace element patterns of the analysed samples are comparable to middle-upper continental crust which might have been inherited from variable magma sources. The Nb/La vs Ba/Rb plot as observed from the samples of Lohit batholith is represented in the Fig.10 The vertical trend between the mantle derived melts and continental crust (Kula Basalt and EMM) suggest assimilation and fractional crystalisation (AFC) of the mantle derived magma rather than sole influence of metasomatism of the mantle wedge by the subduction generated fluids[4,5,45].

Table 1. a-d Major, Trace and REE contents for gabbro, quartz diorite, trondhjemite and leucogranite

Major and trace element compositios of Gabbro										
	Number									
	L41	L43	L49	L58	D31	D40	D59	L51	L52	L57
Major element oxide (wt%)										
SiO_2	40.34	51.96	50.93	47.93	43.99	51.19	49.2	49.56	50.62	49.11
TiO_2	2.47	1.00	0.55	0.95	0.86	1.01	1.23	0.93	0.89	1.3
Al_2O_3	10.4	15.26	16.53	16.77	14.75	16.66	13.39	12.13	12.73	12.81
Fe_2O_3	27.01	11.67	9.85	11.82	17.02	9.77	11.14	15.47	14.74	13.19
MnO	0.46	0.22	0.18	0.20	0.44	0.23	0.24	0.34	0.3	0.25
MgO	7.20	7.47	6.22	5.83	7.66	5	6.03	7.9	6.75	7.67
CaO	8.82	6.68	9.89	9.58	9.95	9.05	14.8	8.36	8.08	8.19
Na_2O	2.48	3.45	3.22	4.07	1.94	4.89	2.6	3.25	3.7	3.22
K_2O	0.31	0.64	0.21	0.37	0.8	0.55	0.52	0.17	0.12	1.63
P_2O_5	1.22	0.31	0.17	0.59	0.29	0.68	0.2	0.07	0.21	0.53
Total	100.73	98.65	97.75	98.11	97.70	99.05	99.36	98.19	98.14	97.89
Na_2O / K_2O	8.00	5.39	15.33	11.00	2.43	8.89	5.00	19.12	30.83	1.98
CaO / Na_2O	3.56	1.94	3.07	2.35	5.13	1.85	5.69	2.57	2.18	2.54
Al_2O_3 / TiO_2	4.21	15.26	30.05	17.65	17.15	16.50	10.89	13.04	14.30	9.85
Trace elements (ppm)										
Ni	49.50	69.21	65.81	66.35	54.11	28.00	85.40	36.50	21.80	123.80
Rb	4.10	49.06	5.97	16.41	33.93	5.50	6.40	2.50	3.50	36.10
Sr	874.80	1438.26	823.75	1755.84	374.50	377.00	197.00	124.00	202.00	435.00
Zr	65.20	30.97	20.31	25.74	36.60	288.00	71.00	47.00	53.00	101.00
Nb	25.50	14.59	1.85	10.80	1.65	7.40	5.70	5.10	4.80	8.80
Ba	104.40	510.37	96.24	366.57	111.81	98.00	20.00	25.00	18.00	274.00
Pb	4.82	38.70	4.76	10.49	7.57	5.20	6.90	1.10	1.80	4.40
Th	0.71	4.73	0.15	0.57	2.14	2.75	0.45	0.21	0.65	2.68
U	0.30	1.55	0.11	0.40	1.12	1.04	0.60	0.09	0.43	0.39
La	46.30	35.25	6.63	33.28	9.27	24.20	3.62	2.14	2.41	23.67
Ce	126.01	82.24	17.17	84.04	22.50	55.52	10.39	5.63	6.36	54.32
Pr	20.78	12.23	2.83	13.21	3.52	7.30	1.82	0.92	1.04	7.50
Er	9.54	6.53	3.87	7.82	11.84	5.28	2.37	1.97	2.19	2.91
Nd	97.09	52.64	14.34	60.08	17.92	30.00	9.29	4.50	5.26	31.43
Dy	18.36	12.20	6.83	14.72	16.72	9.14	4.15	2.83	3.45	5.94
Eu	3.88	3.05	2.00	4.11	1.96	2.12	1.18	0.66	0.82	2.29
Sm	21.29	12.17	4.35	14.00	6.30	7.74	3.02	1.70	1.94	7.80
Ho	3.63	2.51	1.50	3.04	4.11	2.09	0.95	0.75	0.84	1.24
Yb	8.84	6.34	4.08	7.23	15.14	5.56	2.41	2.17	2.36	2.79
Lu	1.26	0.91	0.61	1.04	2.43	0.88	0.38	0.35	0.38	0.44
La/Yb	5.24	5.56	1.63	4.60	0.61	4.35	4.31	0.99	1.02	8.48
Zr/Sm	3.06	2.54	4.66	1.84	5.81	37.21	23.51	27.65	27.32	12.95
Rb/Sr	0.00	0.03	0.01	0.01	0.09	0.01	0.03	0.02	0.02	0.08
Ce/Pb	26.14	2.13	3.61	8.01	2.97	10.68	1.51	5.12	3.53	12.35
(La/Yb)N	1.96	0.41	0.38	0.24	1.12	5.97	10.49	2.19	10.11	2.38
(Yb)N	52.01	37.29	23.98	42.54	89.07	32.71	14.18	12.76	13.88	16.41

Table 1a.

	Major and trace element compositios of quartz diorite													
	Number													
	L45	L56	L67	L75	L77	L78	L79	L76	D21	D29	D36	D61	L65	L80
Major element oxide (wt%)														
SiO_2	53.37	55.27	55.33	56.79	55.53	54.96	55.49	59.64	58.78	58.43	57.5	56.49	58.28	56.04
TiO_2	0.86	0.77	1.06	1.07	0.97	0.95	0.92	0.90	0.66	0.84	1.11	0.81	0.69	0.9
Al_2O_3	14.46	13.96	14.04	13.10	15.32	16.12	15.68	15.19	15.09	11.29	14.02	16.62	15.77	14.38
Fe_2O_3	11.56	9.04	8.68	9.68	9.63	9.45	9.58	8.07	6.99	8.52	7.91	7.64	6.59	9.87
MnO	0.21	0.16	0.17	0.17	0.18	0.17	0.18	0.16	0.13	0.16	0.15	0.13	0.13	0.16
MgO	6.69	7.21	5.79	6.13	5.86	6.38	6.1	3.85	4.1	6.88	5.15	4.26	4.75	5.94
CaO	8.28	5.82	6.15	7.91	6.75	6.34	7.04	6.22	7.99	7.98	8.35	7.44	5.57	6.83
Na_2O	2.80	3.44	3.43	2.87	3.26	3.11	3.2	3.59	3.29	2.57	3.64	4.54	4.16	3.03
K_2O	0.79	1.52	2.13	1.41	1.29	1.52	1.59	1.48	0.54	0.59	0.55	0.42	1.59	1.21
P_2O_5	0.21	0.22	0.58	0.46	0.31	0.28	0.29	0.32	0.23	0.13	0.18	0.46	0.25	0.27
Total	99.25	97.42	97.36	99.61	99.09	99.27	100.07	99.42	97.81	97.41	98.56	98.82	97.79	98.62
Na_2O / K_2O	3.54	2.26	1.61	2.04	2.53	2.05	2.01	2.43	6.09	4.36	6.62	10.81	2.62	2.50
CaO / Na_2O	2.96	1.69	1.79	2.76	2.07	2.04	2.20	1.73	2.43	3.11	2.29	1.64	1.34	2.25
Al_2O_3 /TiO_2	1.25	18.13	13.25	12.24	15.79	16.97	17.04	16.88	22.86	13.44	12.63	20.52	22.86	15.98
Trace elements (ppm)														
Ni	72.47	85.14	60.57	119.42	60.42	58.99	89.01	64.44	0.50	108.50	31.00	0.40	7.10	4.80
Rb	53.03	123.59	311.37	1944.06	93.66	130.98	107.33	103.37	4.30	9.10	6.50	8.80	61.40	23.20
Sr	1019.46	1336.38	#####	1405.81	1613.81	1699.74	1541.51	1484.42	471.00	220.00	351.00	615.00	449.00	470.00
Zr	20.93	16.93	32.31	44.90	45.08	37.39	43.55	44.36	64.00	244.00	122.00	158.00	137.00	251.00
Nb	8.56	12.48	48.57	63.71	19.73	19.41	17.48	27.70	3.70	4.70	5.10	5.00	6.50	6.20
Ba	162.78	1370.18	810.67	948.90	877.17	1220.43	1043.45	1292.18	185.00	35.00	103.00	131.00	336.00	232.00
Pb	8.29	17.33	26.13	35.08	14.37	17.72	15.14	13.66	5.50	5.20	8.00	11.90	16.20	11.10
La	23.41	33.56	85.37	78.02	37.18	29.32	41.66	57.12	6.17	5.62	8.25	13.32	10.42	12.24
Ce	56.39	69.78	193.31	234.86	94.81	80.16	96.70	138.02	14.80	15.90	23.17	29.82	22.60	28.95
Pr	8.83	9.43	22.93	39.22	13.74	12.74	14.16	20.42	2.10	2.40	3.43	3.81	3.16	3.90
Er	8.18	5.32	7.35	11.46	6.58	6.44	6.60	9.14	2.29	2.06	3.46	1.63	1.58	1.81
Th	3.52	6.59	23.26	17.71	4.62	6.24	4.22	17.01	1.60	0.50	1.10	0.55	1.27	1.16
U	1.61	0.69	7.35	15.47	2.55	5.05	3.72	7.96	1.23	0.26	1.20	0.27	0.75	0.40
Nd	40.30	37.28	88.30	169.05	59.40	55.77	60.10	85.77	9.72	10.94	15.92	15.30	13.75	16.03
Dy	14.27	9.20	14.67	24.60	13.01	12.63	13.01	17.87	3.70	3.57	5.78	2.92	2.74	3.27
Eu	2.61	2.52	4.34	8.18	3.67	3.76	3.67	5.25	0.99	1.06	1.97	1.13	1.05	1.10
Sm	10.68	8.61	17.31	35.06	13.51	13.27	13.70	19.32	2.89	3.06	4.71	3.52	3.19	4.06
Ho	3.10	1.99	3.00	4.64	2.66	2.62	2.70	3.69	0.88	0.81	1.33	0.66	0.63	0.73
Yb	8.32	5.44	7.12	9.91	6.36	6.52	6.53	9.30	2.56	2.13	3.61	1.62	1.65	1.73
Lu	1.23	0.79	1.04	1.38	0.94	0.96	0.96	1.35	0.42	0.34	0.57	0.27	0.27	0.27
La/Yb	2.81	6.17	11.99	7.87	5.84	4.49	6.38	6.14	2.41	2.64	2.29	8.22	6.32	7.08
Zr/Sm	1.96	1.97	1.87	1.28	3.34	2.82	3.18	2.30	22.15	79.74	25.90	44.89	42.95	61.82
Rb/Sr	0.05	0.09	0.25	1.38	0.06	0.08	0.07	0.07	0.01	0.04	0.02	0.01	0.14	0.05
Ce/Pb	6.80	4.03	7.40	6.69	6.60	4.52	6.39	2.97	10.10	2.69	3.06	2.90	2.51	1.40
(La/Yb)N	2.02	4.43	8.60	5.65	4.19	3.22	0.44	4.41	1.73	1.89	1.64	5.90	4.53	5.08
(Yb)N	48.93	31.99	41.89	58.31	37.43	38.37	89.07	54.72	15.06	12.53	21.24	9.53	9.71	10.18

Table 1b.

Major and trace element compositios of leucoranite													
	Number												
	D53	L72	L61	L62	L68	L70	L73	D33	L66	L63	D69	D62	D63
Major element oxide (wt%)													
SiO_2	73.77	62.25	79.76	78.76	80.12	73.38	75.19	75.47	75.37	77.06	75.52	74.93	75.06
TiO_2	0.45	0.73	0.03	0.03	0.16	0.26	0.11	0.40	0.15	0.06	0.36	0.41	0.21
Al_2O_3	12.99	14.80	11.37	12.37	10.86	14.73	12.63	13.21	12.24	12.73	14.23	12.69	13.51
Fe_2O_3	3.79	5.69	0.55	0.58	1.19	2.23	1.00	3.47	1.81	0.98	2.88	2.70	1.58
MnO	0.12	0.11	0.06	0.05	0.05	0.07	0.03	0.05	0.04	0.01	0.05	0.04	0.04
MgO	0.93	4.58	0.12	0.08	0.29	0.59	0.23	0.78	0.46	0.12	0.80	0.86	0.53
CaO	3.83	3.78	0.84	1.08	1.3	1.77	1.43	3.62	1.7	0.69	2.74	2.32	1.79
Na_2O	4.50	3.42	4.62	4.07	3.34	4.11	3.40	4.86	3.81	3.63	3.85	3.24	3.11
K_2O	0.34	2.24	3.16	3.98	3.61	3.93	4.05	0.30	3.45	5.19	3.49	3.64	4.80
P_2O_5	0.18	0.39	<0.01	<0.01	0.05	0.10	0.06	0.12	0.06	0.01	0.28	0.31	0.20
Total	100.89	97.98	100.51	100.99	100.95	101.17	98.14	101.28	99.1	100.48	101.21	101.13	100.84
Na_2O / K_2O	13.24	1.53	1.46	1.02	0.93	1.05	0.84	16.20	1.10	0.70	1.10	0.89	0.65
CaO / Na_2O	0.85	1.11	0.18	0.27	0.39	0.43	0.42	0.74	0.45	0.19	0.71	0.72	0.58
Al_2O_3 / TiO_2	28.87	20.27	379.00	412.33	67.88	56.65	114.82	33.03	81.60	212.17	39.53	30.95	64.33
Trace elements (ppm)													
Ni	19.00	38.09	11.30	17.36	17.69	16.30	12.47	15.00	BDL	BDL	33.69	24.27	30.85
Rb	25.77	312.39	234.41	425.21	487.20	449.05	509.44	15.41	88.30	100.80	390.62	416.56	421.00
Sr	469.68	1632.15	356.61	220.85	1129.05	1161.63	1087.14	405.96	281.00	244.00	1705.16	1429.72	1439.77
Zr	12.14	5.53	6.48	15.97	14.36	5.58	7.19	14.30	72.00	45.00	14.4	17.6	17.2
Nb	5.14	20.76	12.77	26.89	38.26	35.13	16.27	16.63	10.00	3.30	37.6	49.2	48.1
Ba	88.76	1982.37	2518.36	67.51	3452.71	3802.33	2646.36	82.51	594	852	2816.2	3870.4	4355.3
Pb	6.46	29.34	93.11	109.56	88.29	79.93	90.15	5.14	22.8	34.3	79.7	65.0	95.4
La	14.01	57.01	18.46	8.97	102.13	153.67	107.97	22.79	16.42	26.75	170.8	644.3	697.5
Ce	44.60	109.42	43.65	21.47	212.50	666.18	210.06	67.01	29.95	47.78	633.0	1229.6	1297.1
Pr	8.33	12.12	5.48	2.82	27.01	31.53	24.33	11.77	3.15	4.95	32.6	62.8	65.8
Er	32.04	2.57	1.06	1.94	6.22	4.03	2.33	17.82	0.59	0.52	3.0	4.2	5.7
Th	2.26	6.07	15.36	25.99	108.20	10.79	59.13	1.91	10.30	18.34	74.1	120.8	176.3
U	1.76	2.05	6.74	18.43	16.13	4.73	4.09	0.50	1.71	1.71	20.1	11.4	59.8
Nd	46.97	42.33	21.36	11.38	99.56	112.84	83.05	60.05	10.72	15.97	102.4	189.9	197.8
Dy	50.62	5.21	2.84	3.61	14.08	8.77	5.84	32.97	1.20	1.10	5.11	7.34	9.60
Eu	4.25	2.84	1.10	0.64	3.72	3.16	2.50	3.98	0.52	0.76	3.3	5.0	5.0
Sm	19.44	7.62	6.95	3.62	22.21	18.88	14.66	19.25	2.05	2.76	13.4	22.5	24.3
Ho	11.74	1.04	0.44	0.72	2.54	1.60	0.97	7.01	0.25	0.22	1.01	1.36	1.88
Yb	35.21	2.23	1.00	2.07	5.42	3.12	1.56	17.69	0.56	0.46	2.91	3.79	5.83
Lu	5.20	0.34	0.14	0.29	0.73	0.27	0.21	2.50	0.08	0.07	0.47	0.58	0.91
La/Yb	0.40	25.53	18.55	4.34	18.85	49.18	69.42	1.29	29.32	58.15	58.63	170.20	119.67
Zr/Sm	0.62	0.73	0.93	4.41	0.65	0.30	0.49	0.74	35.12	16.30	1.08	0.78	0.71
Rb/Sr	0.05	0.19	0.66	1.93	0.43	0.39	0.47	0.04	0.31	0.41	0.23	0.29	0.29
Ce/Pb	3.73	0.47	0.20	2.41	8.33	2.33	13.04	1.31	1.39	7.94	18.91	13.60	2.69
(La/Yb)N	18.31	13.30	3.11	13.52	35.27	49.79	21.03	41.71	42.05	122.08	219.16	85.84	0.92
(Yb)N	13.14	5.86	12.16	31.88	18.38	9.15	3.29	2.71	17.14	22.27	2.66	34.28	104.03

Table 1c

Major and trace element compositios of Trondhjemite					
	Nmber				
	L55	L59	D22	D46	D65
Major element oxide (wt%)					
SiO_2	64.12	69.11	65.49	74.05	71.79
TiO_2	0.46	0.45	0.3	0.13	0.08
Al_2O_3	16.15	15.05	18.3	16.11	14.92
Fe_2O_3	4.02	2.00	1.48	1.12	0.86
MnO	0.08	0.03	0.02	0.02	0.01
MgO	4.09	1.12	0.59	0.55	0.26
CaO	4.79	2.02	4.97	3.55	4.01
Na_2O	5.02	3.30	5.78	4.70	4.96
K_2O	1.46	4.54	0.67	0.61	0.39
P_2O_5	0.23	0.17	0.13	0.01	0.11
Total	100.42	97.79	97.74	100.84	97.39
Na_2O / K_2O	3.44	0.73	8.63	7.70	12.72
CaO / Na_2O	0.95	0.61	0.86	0.76	0.81
Al_2O_3 / TiO_2	35.11	33.44	61.00	123.92	186.50
Ni	147.77	18.80	BDL	22.14	BDL
Rb	90.64	547.88	15.20	40.94	2.90
Sr	1976.04	1557.78	1099.00	2634.82	583.00
Zr	11.68	11.50	101.00	8.15	293.00
Nb	6.52	4.33	7.30	3.54	1.90
Ba	1330.46	2946.86	284.00	1286.20	101.00
Pb	25.75	223.73	19.5	36.2	6.50
La	12.37	138.10	6.36	4.69	4.81
Ce	28.06	602.10	13.2	7.8	9.83
Pr	4.06	31.06	1.8	0.8	1.1
Er	2.05	1.19	1.14	0.16	0.29
Th	2.01	74.50	1.94	0.16	1.46
U	1.58	5.74	2.34	0.20	0.41
Nd	18.01	102.08	7.44	2.80	3.81
Dy	4.00	2.77	2.24	0.28	0.51
Eu	1.60	3.74	1.34	1.39	0.55
Sm	5.17	16.50	2.37	1.06	0.74
Ho	0.81	0.38	0.49	0.06	0.12
Yb	1.94	0.45	1.19	0.16	0.31
Lu	0.27	0.06	0.17	0.03	0.05
La/Yb	6.37	305.54	5.34	29.72	15.52
Zr/Sm	2.26	0.70	42.62	7.69	395.95
Rb/Sr	0.05	0.35	0.01	0.02	0.00
Ce/Pb	1.09	0.22	0.68	1.51	3.61
(La/Yb)N	10.35	35.55	7.95	22.75	4.61
(Yb)N	11.43	2.64	7.00	0.94	1.82

Table 1d.

Table 2. Rb, Sr concentrations and $^{87}Sr/^{86}Sr$ ratios of selected samples of Lohit batholith

Samples	Longitude	Latitude	Rock type	Rb(ppm)	Sr(ppm)	$^{87}Rb / ^{86}Sr$ (atomic)	$^{87}Sr/^{86}Sr$ (atomic)
L-72	28°20′32″	97°10′41″	Diorite	8.86	113.775	0.208±2%	0.704671±0.0002
L-45	28°02′14″	96°56′55″	Diorite	174.98	120.608	5.683±2%	0.703876±0.0003
L-70	28°18′20″	97°06′25″	Granodiorite	121.09	314.04	1.116±2%	0.707093±0.0003
L-71	28°19′43″	97°08′48″	Granodiorite	53.94	346.44	0.4503±2%	0.704698±0.0002
L-69	28°15′44″	97°01′38″	Granite	66.08	89.149	1.6795±2%	0.714987±0.0001
D-62	28°50′78″	96°50′48″	Diorite	104.55	201.49	1.5009±2%	0.705863±0.0002
D-63	28°50′77″	96°50′45″	Granite	113.2	139.902	2.34072±2%	0.706152±0.0002
D-69	28°50′78″	96°50′50″	Granodiorite	108.29	411.82	0.76061±2%	0.705601±0.0003

4.2. Magma Source

Geochemical details provide evidences for magma sources for three distinct suit of rocks present in the area: (i) gabbro-quartz diorites (ii) trondhjemites and (iii) leocgranites. In all three suits crustal contamination in subduction environment is depicted by the Nb/La – Ba/Rb plots (Fig.10)[4]. Trace element ratios more specifically the HFSE (e.g. Nb, Ta, Ti) are highly sensitive to varying degrees of partial melting of the source. For subalkaline rocks of the area, the degree of partial melting is expected to be high. Therefore, ratios of the incompatible elements may reflect the source characteristics[3]. However, compared to degree of partial melting in intraoceanic arcs on thin lithosphere, the partial melting is lowest in continental arcs on thick lithosphere[36]. Under this condition, melting of the mantle wedge is triggered by addition of the fluids from the subducting slab, where depletion of the mantle wedge post dates the fluid addition. An interesting implication emerging from the study indicate that the residual garnet in the anatectic events can give rise to appropriate high/ heavy REE and HFSE/ REE fractionation. This is evident as there is no strong Nb depletion in these rocks (Figs.6a-d)[5]. Replenishment of the mantle wedge takes place by flux of the LIL enriched materials from the subducting slab[27]. The gabbro-quartz diorite suit is characterized by LREE enrichment, high content of Al_2O_3, Ba and Sr and low contents of Yb. These features suggestive of a source with residual garnet, amphibole or pyroxene and little olivine and plagioclase (i.e. no Eu anomaly). Partial melting of an enriched source melts with high values of Sr and Ba and LREE especially when the degree of partial melting is low[11,23]. On primitive mantle normalized diagram gabbro and quartz diorites display strong Nb and Zr depletion indicating the fact that partial melting is contaminated by contributions of ancient crustal material combined with low SiO_2 contents (40.34 to 51.96 wt%) and low $^{87}Sr/^{86}Sr$ ratios (0.703). This indicates that these rocks should be derived from a metasomatic lithospheric mantle source[53]. However, in quartz diorites, given the fact that SiO_2 and MgO are negatively correlated, fractional crystalisation of the mantle derived basaltic magma might have taken place. This magma is assimilated at different proportions by lower crustal material. Therefore, gabbro enclaves within quartz diorites should represent the original basaltic parent magma with low initial $^{87}Sr/^{86}Sr$ ratios. There is a systematic depletion of TiO_2, Fe_2O_3, MgO and CaO from gabbro to quartz diorites with increasing SiO_2 (Table 1.a-d). This indicates hornblende fractionation. With the strong positive Sr anomalies and insignificant Eu anomalies plagioclase fractionation became insignificant when differentiation progressed to an advanced stage[53]. With higher values of Al_2O_3, Na_2O, P_2O_5 and Rb contents and enriched LREE and HREE, leucogranites are characterized as forming from crustal melts[10]. Leucogranites are also chracterised by high $^{87}Sr/^{86}Sr$ ratio (0.714987). Although in the previous model[16], the water pressure condition for occurrence of tourmaline bearing leucogranite was emphasized, in the present study, it is found that the leucogranites in the Yasong and Dambuin area (northeastern part of the batholith) are biotite leucogranites rather than tourmaline leucogranites. This negates the high water pressure condition especially for the formation of the leucogranites. Trondhjemites are high in Zr/Sm and La/Yb (Table -1). This indicates garnet stabilization at the deeper part of the crust, which is responsible for the changes of the composition of the melt along with the high value of Si and gradual decrease of Fe, Mg and Yb values[20]. These melts may also be characterised by more sodic and more aluminous[5]. On the other hand, no negative Eu anomaly in trondjhemite indicate that plagioclase is almost nil in the solid residue to deplete the melt in Sr and Eu. Therefore garnet bearing source may account for the geochemical variability obtained for the batholiths.

5. Conclusions

The majority of the granitoids of Lohit batholith are metaluminous and only a few of them are peraluminous. Therefore these granitoids can well be characterized as I-type granitoids. Major and trace element geochemistry of these granitoids indicate both lithosperic and asthenospheric mantle components where the parental mafic magmatic melts evolve to granodioritic or leucogranitic composition specially towards the eastern part. This also indicate involvement of crustal derived melts in the eastern part. The crustal signature in these rocks suggests simultaneous assimilation of the upper to mid crustal rocks and the fractional crystallisation of the mantle derived meltstowards the thicker continental crust in the eastern part. Involvement of the crustal melt is also reflected in the isotopic characteristics with higher Sr isotopic values in the eastern part.

Mantle melting was initiated by fluid injection from the subducting mantle and as a result the mantle wedge is replenished. Fractional crystalisation of the mantle derived magma assimilated with the lower crustal material provided the source for the gabbro-quartz diorite sequence of the Lohit batholith. The early melt through the thin wedge could not fractionate much and therefore the Sr isotopic ratio in the gabbro -quartz -diorite sequence is very low (0.703), which represents very lowly fractionated mantle composition. In the eastern part of the batholith, the temporal variation in the magma genesis is reflected in the chemical characteristics and in the Sr isotopic ratio. The more fractionated and evolved leucogranite of the eastern part shows a rapid increase in the Sr isotopic initial ratio of 0.714. Higher Sr isotopic and La /Yb ratio, higher value of P and decrease in Nb, Zr, Ta and Yb in the eastern part indicate that the younger phases are derived from a depleted mantle later enriched by the process of metasomatism.

ACKNOWLEDGEMENTS

The author is grateful to Department of Science and Technology, New Delhi, for financial assistance (Project No.ESS/16/242/2005/SIANG-LOHIT/06). The author acknowledges the help received from IIT Roorkee Isotope Geology Lab and analytical lab of Wadia Institute of Himalayan Geology, Dehradun. The author is grateful to anonymous reviewer for the comments, which helped improvement of the manuscript considerably.

REFERENCES

[1] Acharyya, S.K. 1982. Structural framework and tectonic evolution of the Eastern Himalaya. Himalayan Geology, 10:412-419

[2] Acharyya, S.K. 1987. Cenozoic plate motions creating the Eastern Himalayan and Indo-Burmese Range around the northeast corner of India. In: Ghosh, M.C. & Varadarajan, S. (Eds.) Amphibolites and Indian Plate Margins Patna University Patna 143-160

[3] Ahmed T., Thakur, V.C., Islam, R., Khanna, P.P., and Mukherjee, P.K. 1998. Geochemistry and geodynamic implications of magmatic rocks from the Trans –Himalayan arc. Geochemical Journal, 32:383-404

[4] Altunkayanak, S., Dilek, Y., Genc, C.S., Sunal, G., Gertisser, R., Furnes, H., Foland, K.A., and Yang J. 2012. Spatial, temporal and geochemical evolution of Oligo-Miocene granitoid magmatism in western Anatolia. Turkey. Gondwana Research, 21: 961-986 doi:10.1016/j.gr.2011.10.010

[5] Altunkayanak, S., Rogers, N.W., and, Kelley, S.P. 2010. Causes and effects of geochemical variation in Late Cretaceous volcanism in te Folca Volcanic Centre (NW anatoli, Turkey), International Geology Review, 52:579-607

[6] Arculus, R.J. 1994. Aspects of magma genesis in arcs, Lithos 33, 189-208.Ayres, M and Harris, N (1997) REE fractionation and Nd-isotope disequilibrium during crustal anatexis: constraints from Himalayan leucogranites. Chemical Geology, 139: 249-269

[7] Bhalla, J.K., Srimal, N., and Bishui, P.K. 1990. Isotopic study of Mishmi Complex, Arunachal Pradesh, NE Himalaya, Record Geological Survey of India. 123 (2) 20-21

[8] Coward, M.P., Jan, M. Q., Rex, D, Tarney, J., Thirlwall, M., and Windley, B.F. 1982. Geotectonic framework of Himalaya in North Pakistan. Jour.Geol.Soc.London, 130, 299-308

[9] Debon, F., LeFort, p., Sheppard, S.M.F and sonnet, J. 1986. The four plutonic belts of the Trans-Himalaya: A chemical, mineralogical, isotopic and chronological synthesis along the Tibet-Nepal Section, Jour. Petr., 27, 219-250

[10] Deitrich , V.J., Frank, W., and Honnegar,K. 1983. A Jurassic-Cretaceous island arc in Ladakh Himalaya, Jour Volcan.Geotherm. Res., 18,405-433

[11] Dilek, Y., and Altunkayanak, S. 2010. Geochemistry of Neogene-Quaternary alkaline volcanism in western Anatolia turkey and implications for the Aegean mantle, International Geology Review, 52 : 631-655

[12] Gibson, S.A., Thompson, R.N., Leonardos, O.H., Dickin, A.P. and, Mitchel, J.G. 1995.The Late Cretaceous impact of the Trindade mantle plume: evidence from large –volume, mafic, potassic magmatism in in SE Brazil, Jornal of Petrology, 36:189-229

[13] Goswami, T.K. 2013. Geodynamic significance of leucogranite intrusion in the Lohit batholith near Walong, Arunachal Pradesh, India, Current Science, 104 : 229-234

[14] Gururajan, N.S., and Chowdhury, B.K. 2003. Geology and tectonic history of the Lohit Valley, Eastern Arunachal Pradesh India, Journal of Asian Earth Sciences, 21: 731-741

[15] Gururajan, N.S., and Chowdhury, B.K. 2007. Geochemistry and tectonic implications of the Trans- Himalayan Lohit Plutonic Complex, Eastern Arunachal Pradesh. Journal of Geological Society of India, 70:17-33

[16] Gururajan, N.S., and Chowdhury, B.K. 2009. Geology and structural evolution of the eastern Himalayan Syntaxis. Journal of Himalayan Geology, 30:17-34.

[17] Gursu, S., and Goncuoglu, M.C. 2008. Petrogenesis and geodynamic evolution of the Late Neoproterozoic Post-collisional felsic magmatism in NE Afyon area. Western Central Turkey, Geological Society of London Special Publication, 297: 409-431

[18] Harangi, S., Vaselli, O., .Tonarini, S., Szabo, C., Harangi, R.,and Coradossi, N. 1995. Petrogenesis of Neogene extension related alkaline volcanic rocks of the Little Hungarian Plain Volcanic Field (Western Hungary).In Downes, H. and Vaselli, O (eds) Neogene and related magmatism in the Capatho-Panonian region, Acta Volcanologica, 7:173-187.

[19] Harris, N.B.W., Pearce, J. A., Tindle, A.G. 1986 geochemical characteristics of collision –zone magmatism, Grol.Soc. Lond.Sp.Publ.,19,67-81.

[20] Hasachke, M.R. 2002. Evolutionary geochemical patterns of Late Cretaceous to Eocene arc magmatic rocks in North Chile: implications for Andean crustal growth. EGU Stephan Mueller Special Publication Series 2:207-218.

[21] Honeggar, J., Dietrich, V., Frank, W., Gansser, S., Thoni, M. and Trommsdrof, V. 1982 Magmatism and metamorphism in the Ladakh Himalaya (the Indus- Tsangpo Suture Zone), Earth.Planet. Sci. Lett, 60, 253-93.

[22] Jain, A.K., Singh, S., and Manickavasagam, R.M. 2002. Himalayan Collision Tectonics, Gondwana Research Group Memoir, 7:114pp.

[23] Jiang, Y.H., Jiang, S.Y., Ling, H.F., and Dai, B.Z. 2006. Low-degree melting of a metasomatised mantle origin of Cenozoic Yulong monzogranite-porphyry, east Tibet: geochemical and Sr-Nd-Pb-Hf isotopic constraints. Earth and Planetary Science Letters, 241: 617-633

[24] Khanna, P.P., Saini, N.K., Mukherjee, P.K., and Purohit, N.K. 2009. An appraisal of ICP-MS technique for determination of REEs: long term QC assessment of silicate rock analysis, Himalayan Geology, 30: 95-99

[25] Kovarikova, P., Siebel, W., Jelinek, E., Stemprok, M., Kachlik, V., Holub, F.V., and Blecha, V. 2010. Dioritic intrusions of the Slavkovsky les (Kaiserwald), Western

Bohemia: their origin and significance in late Varsican granitoid magmatism, International Journal of Earth Science (Geol Rundsch), 99:545—565.

[26] Kumar, G. 1997. Geology of Arunachal Pradesh, Geological Society of India.

[27] Kumar, R., Lal, N., Singh, S., and Jain, A.K. 2007. Cooling and exhumation of the Trans-Himalayan Ladakh Batholith as constrained by fission track apatite and zircon ages, Current Science, 92: 490-496

[28] Lucas-Tooth, H., and Pyne, C. 1964. Advances in X-Ray Analysis, New York: Plenum Press, 7:523p.

[29] Martin, H. 1999. The adakitic magmas: Modern analogues of Archean Ganitoids, Lithos, 46:411-429

[30] Mc Culloch, M.T., and Gamble, J.A. 1991. Geochemical and geodynamical constraints on subduction zone magmatism, Earth and Planetary Science Letters, 102:358-374.

[31] Middlemost, E.A.K. 1994. Naming minerals in the magma/igneous rock system, Earth Science Review, 37:215-224 doi 10,1016 /0012-8252(94)90029-9

[32] Miller, D.M., Goldstein, S.L., and Langmuir, C.H. 1994. Cerium/lead and lead isotope ratios in arc magmas and enrichment of lead in the continents. Nature, 368:514-519

[33] Mishra, D.K. 2009. Litho-tectonic Sequence and their Regional Correlation along the Lohit and Dibang Valleys, Eastern Arunachal Pradesh, Journal of Geological Society of India, 73:213-219

[34] Mitchel, A.H.G. 1981: Phanerozoic plate boundaries in the mainland SE Asia, the Himalaya and Tibet. Journal of Geological Society of London, 152:689-701.

[35] Nandy, D.R. 1976. The Assam Syntaxis of the Himalaya-A reinterpretation, Geological Survey of India, Miscellaneous Publication 24:363-367.

[36] Pearce, J.A., Parkinson, I.J. and, Peate, D.W. 1994. Geochemical evidence for magma generation above subduction zones (Abst), Goldschmidt Conference, Edinburgh, pp.701-702

[37] Peccerillo, A., and Taylor, S.R. 1976. Geochemistry of Eocene Calc-alkaline volcanic rocks from Kasta Manonu area, Turkey, Contribution to Mineralogy and Petrology, 58:39-63 doi:10,1007/BF 00384745

[38] Roland, Y., Pecher, A. and Picard, C.2000 Middle Cretaceous back-arc formation and arc evolution along the Asian margin: the Shyok Suture Zone in northern Ladakh (NW Himalaya), Tectonophysics, 325, 145-173

[39] Shand, S.J. 1927. The Eruptive Rocks. John Wlley, New York

[40] Sharma, K.K., Chaube, V.M., and Chatti, H.R. 1991. Geological setting of the ophiolites and magmatic arc of the Lohit Himalaya (Arunachal Pradesh), with special reference to their petrochemisty, International Geology and Geodynamic evolution of the Himalayan collision zone., Physics and Chemistry of the Earth, Pergamon Press, PLC. 4:149-163.

[41] Saini, N.K., Mukherjee, P.K., Rathi, M.S., Khanna, P.P., and Purohit, K.K. 1998. A new geochemical reference sample of granite (DH-G) from Dalhousie Himachal Himalaya, Journal of Geological. Society of .India, 52:602-606

[42] Singh, S., and Chowdhury, P.K. 1990.An outline of the Geological framework of the Arunachal Himalaya. Journal of Himalayan Geology, 1:189-197.

[43] Singh, S.,and Jain , A.K. 2002. Himalayan Granitoids. Journal of Virtual Explorer, 1-20

[44] Singh, S. 1993. Geology and tectonic evolution of the Eastern Syntaxial Bend, Arunachal Himalaya. Journal of Himalayan Geology, 42 :149-163

[45] Tatsumi, Y., Hamilton, D.L., and Nesbitt, R.W. 1986. Chemical characteristics of fluid phase related from a subducted lithosphere and origin of arc magmas: evidence from high presuure experiments and natural rocks, Journal of Volcanology and Geothermal Research, 29:293-309

[46] Thakur, V.C., and Jain, A.K. 1975. Some observation on deformation, metamorphism and tectonic significance of rocks of some parts of Mishmi hills, Lohit District (NEFA) Arunachal Pradesh, Journal of Himalayan Geology, 5: 339-364

[47] Thakur,, V.C. 1993. Geology of the Western Himalaya. Pergamon Press,Oxford and New York, 355pp.

[48] Trivedi, J.R. 1990. Geochronological studies of the Himalayan Granitoids. Unpublished PhD thesis, Gujrat University, 170pp

[49] Trivedi, J.R., Gopalan, K., and Valdiya K.S. 1984. Rb-Sr ages of granitic rocks within the Lesser Himalayan nappes, Kumaun, India, Journal of Geological Society of India, 25:641-654

[50] Thuy, N.T.B., Satir, M., Siebel ,W., Vennemann,T., and Long, T.V. 2004. Geochemical and isotopic constraints on the petrogenesis of granitoids from Dalat zone, southern Vietnam, Journal of Asian Earth Sciences, 23:467-482

[51] Weinberg R.F. and Searly, M.P. 1998 the Pangong injection complex, Indian Karakoram: a case pf pervasive granite flow through hot viscous crust. Jour Geol. Soc. London, 155,883-891.

[52] Yang, J.H., Wu, F.Y., Chung, S.L., Chung, S.L., Wilde, S.A., and Chu, M.F. 2004. Multiple ource for the origin of granites: geochemical and Nd/Sr isotopic evidence from the Gudaling granite and its mafic enclaves, north east China, Geochimica et Cosmochimica Acta, 68:4469-4483

[53] Yin, A. 2006. Cenozoic tectonic evolution of the Himalayan orogen as constrained by along strike variation of structural geometry, exhumation history and foreland sedimentation. Earth Science Review, 1-131

[54] Zhang,, S.H., Zhao, Y., Kroner, A., Liu, X.M., Xie, L.W., and Chen, F.K. 2009. Early Permian plutons form the North China Block: constraints on continental arc evolution and convergent margin magmatism related to the Central Asian Orogenic Belt, International Journal of Earth Sciences (Geol Rundsch) 98:1441-1467